THE ASTROPHYSICAL JOURNAL, 245:1094–1109, 1981 May 1

NEUTRINOS IN GRAVITATIONAL COLLAPSE. I. ANALYSIS OF TRAJECTORIES

S. V. DHURANDHAR AND C. V. VISHVESHWARA
Raman Research Institute, Bangalore-560 080, India
Received 1980 June 13; accepted 1980 September 23

ABSTRACT

The behavior of neutrinos is investigated in a collapsing object. The model considered consists of the Friedmann dust interior matched onto the Schwarzschild exterior. The neutrino trajectories are taken to be null geodesics, the geometric optics approximation being valid for the relevant energy range. The matter is assumed to be transparent to the neutrinos.

We first compute the null geodesics in both the geometries appropriately matched at the boundary. We then derive an expression for the spectral shifts of the neutrino. We study in detail the properties of backward emission and the confinement of the neutrinos to the vicinity of the collapsing object at various stages of collapse. The analysis leads to a rather interesting and complex pattern in the evolution of the process of confinement as the collapse progresses.

Subject headings: dense matter — neutrinos — stars: collapsed

I. INTRODUCTION

Of late the role of neutrinos in compact objects and in supernova explosions has been recognized to be of prime importance. It is believed that the neutrinos act as carriers of energy from the core to the envelope of the supernova. This is possible because the interaction between the neutrinos and the matter through which they pass is negligible and to a good approximation they can be treated as free particles. However, when one is interested in situations where the gravitational field is sufficiently strong, the neutrinos would react appreciably to this field although they may be free from other interactions. Under these circumstances the gravitational field is prescribed by the general theory of relativity. A general relativistic description of neutrino transport in spherically symmetric, static, compact objects has been given by Kembhavi and Vishveshwara (1981). Their treatment is semiclassical in that they have studied the perturbative solutions of the massless Dirac equation in the Schwarzschild interior and exterior metrics. Their calculations show that neutrinos may be trapped in sufficiently strong gravitational fields. Such a trapping could have astrophysical relevance—this could reduce the available energy.

In this paper we investigate the behavior of neutrinos in another general relativistic situation of astrophysical significance, namely gravitational collapse. We assume that a star undergoes geodesic gravitational collapse and emits neutrinos at advanced stages of collapse. We expect neutrino trapping to be enhanced in the present case as compared to that of the static star, since the collapse will tend to further inhibit the neutrinos from going to infinity. In the range of relevant energies, the effect of gravitation on the neutrinos can very well be described in the geometric optics limit and hence the latter can be assumed to move along null geodesics in the background geometry. We examine the neutrino trajectories in detail, especially their escape and confinement relative to observers stationed at infinity. In general the confined neutrinos circle around the collapsing star and fall into the eventually formed black hole. This analysis and the techniques employed can be utilized in studying the neutrinos emitted in any specific astrophysical model of collapse. Furthermore, these computations are needed in obtaining the flux profile of the energy carried away by the neutrinos. Evidently, this issue is even more complex owing to the redshift, the time of flight, and other effects involved. Calculations and results pertaining to those considerations will be published in a separate paper.

We remark at this stage that though the investigation involves null geodesics, the case of the neutrinos is quite different from that of photons, where one must assume them to be emitted from the surface of the star. The star material is transparent to the neutrinos; hence they could be emitted anywhere from the interior of the object and received outside. We must therefore take into account both the interior and the exterior geometry of the star properly matched at the boundary. This engenders radically new effects which would be absent in the treatment of photons.

II. THE INTERIOR AND THE EXTERIOR GEOMETRIES

We assume that the star collapses under its own gravitational pull and that the entire situation possesses spherical symmetry. Further, the density ρ and pressure p are taken to be functions of time alone. It is well known then that the geometry of the interior of the star is described by the Robertson-Walker line element with $k = +1$. The exterior geometry is Schwarszchild by Birkhoff's theorem. Our aim is to study the behavior of null geodesics in both these geometries, which are appropriately matched at the stellar surface.

The interior geometry of the collapsing star is described by the following line element:

$$dS^2 = dT^2 - S^2(T)[(1 - \alpha R^2)^{-1} dR^2 + R^2(d\theta^2 + \sin^2 \theta d\varphi^2)] , \tag{2.1}$$

where

$$\alpha = 2m/R_b{}^3 .$$

We have chosen to work in geometrized units in which $c = 1$ and $G = 1$. Here m is the mass of the star and R_b the R-coordinate of a particle on the boundary, while $S(T)$ is the expansion factor.

If $p \ll \rho$, we can set $p = 0$ identically to a very good approximation. Every particle in the star then describes an infalling radial geodesic, i.e., the collapse is geodetic. The resulting interior geometry is represented by the Friedmann dust metric and the expansion factor satisfies the equation,

$$\left(\frac{dS}{dT}\right)^2 = \alpha \frac{1 - S}{S} . \tag{2.2}$$

The maximum value of $S(T)$ is unity. The spatial coordinates (R, θ, φ) of a particle remain constant during the collapse, and only the expansion factor $S(T)$ varies.

The external geometry is Schwarzschild and is given in the usual form by

$$ds^2 = \left(1 - \frac{2m}{r}\right)dt^2 - \left(1 - \frac{2m}{r}\right)^{-1} dr^2 - r^2(d\theta^2 + \sin^2 \theta d\varphi^2) . \tag{2.3}$$

Since our geodesics are going to emanate from some point in the Robertson-Walker geometry and then emerge in the Schwarzschild domain at the surface of the star, we have to break up our discussion into three parts: (*a*) null geodesics in the Robertson-Walker geometry; (*b*) the matching at the surface of the object; (*c*) null geodesics in the Schwarzschild geometry.

The last topic and the matching of geometries at the interface have been extensively discussed in the literature by Misner, Thorne, and Wheeler (1973) and Hoyle and Narlikar (1964). We will briefly discuss the relevant portions applicable to our problem. However, the first topic deserves detailed analysis. We will treat these aspects with due detail in the following section.

III. NEUTRINO TRAJECTORIES

a) Null Geodesics in the Interior Geometry

We can clearly see from relations (2.1) and (2.3) that spherical symmetry is present, therefore without loss of generality we may choose the $\theta = \pi/2$ plane to study the behavior of the null geodesics. Either from symmetry considerations or from the Euler-Lagrange equations we can immediately write down the first integrals:

i) $$S \frac{dT}{d\lambda} = \Gamma ;$$

ii) $$R^2 S^2 \frac{d\varphi}{d\lambda} = h ;$$

iii) $$ds = 0 . \tag{3.1}$$

The last integral arises because the neutrino world line is null. The constants Γ and h are the unscaled measures of the energy and the angular momentum of the neutrino. Since the neutrino trajectory is null, the affine parameter λ may be rescaled, and therefore only the ratio $h/\Gamma = B$ is sufficient to determine the null geodesic. The quantity B may be called the impact parameter of the null geodesic in the interior geometry. Note that B is *not* the impact parameter as measured by an observer at infinity stationed in the Schwarzschild geometry. A relation exists between B and the Schwarzschild impact parameter b for the same null geodesic. We will discuss this point at a later stage.

The equations (i), (ii), and (iii) can be used to obtain the relation

$$S^2\left(\frac{dR}{dT}\right)^2 = (1 - \alpha R^2)\left(1 - \frac{B^2}{R^2}\right) . \tag{3.2}$$

We see that the null geodesics with $B \neq 0$ cannot reach the center of the object $R = 0$, but rather experience a bounce at $R = B$. The qualitative behavior of the geodesics could be studied with the help of the effective potential $V_{\text{eff}} = 1/R^2$. We do not do so here. We write equation (3.2) in terms of the expansion factor S using (2.2):

$$\frac{\alpha^{1/2} dR}{[(1 - \alpha R^2)(1 - B^2/R^2)]^{1/2}} = \pm \frac{dS}{[S(1 - S)]^{1/2}} . \tag{3.3}$$

It is convenient to describe the collapse in terms of a parameter χ given by $S = \cos^2 \chi$. Integrating (2.2) with this substitution yields a relation connecting T and χ,

$$T = \frac{1}{\alpha^{1/2}} (\chi + \sin \chi \cos \chi) . \tag{3.4}$$

Also if we let the neutrino start at $\chi = \chi_0$ and from $R = R_0$, then (3.3) may be integrated:

$$\chi = \chi_0 \pm \frac{1}{4}\left(\sin^{-1} \frac{1 + \alpha B^2 - 2\alpha {R_0}^2}{1 - \alpha B^2} - \sin^{-1} \frac{1 + \alpha B^2 - 2\alpha R^2}{1 - \alpha B^2} \right), \tag{3.5}$$

where the sign outside the bracket is the same as the sign of $dR/d\chi$. For an outward moving neutrino $dR/d\chi > 0$.

We now express B in terms of the angle the neutrino makes with the radially outward direction as measured by a comoving observer instantaneously coinciding with the neutrino trajectory at R_0. Let ψ_0 be the required angle; then from local differential geometry we have the following relation:

$$\frac{SR_0 d\varphi}{S(1 - \alpha {R_0}^2)^{-1/2} dR} = \tan \psi_0 . \tag{3.6}$$

Then using (3.1) we have

$$B = R_0 \sin \psi_0 . \tag{3.7}$$

From (3.7) we observe that as B is a constant, the expression $R \sin \psi$ is constant along the null geodesic. The epoch angle χ then may be expressed in terms of χ_0, R_0, and ψ_0. From (3.5) and (3.7) we have

$$\chi = \chi_0 \pm \tfrac{1}{4}[\chi_1(R_0) - \chi_1(R)] , \tag{3.8}$$

where

$$\chi_1(R) = \sin^{-1} \frac{1 + \alpha {R_0}^2 \sin^2 \psi_0 - 2\alpha R^2}{1 - \alpha {R_0}^2 \sin^2 \psi_0} .$$

Let χ_b be the epoch when the neutrino emitted with initial parameters χ_0, R_0, and ψ_0 reaches the surface $R = R_b$; then from (3.8) we have the following relations:

For $\psi_0 \leq \pi/2$, $(dR/d\chi|_{R=R_0} \geq 0)$,

$$\chi_b = \chi_0 + \tfrac{1}{4}[\chi_1(R_0) - \chi_1(R_b)] . \tag{3.9}$$

For $\psi_0 \geq \pi/2$, $(dR/d\chi|_{R=R_0} \leq 0)$,

$$\chi_b = \chi_0 + \frac{\pi}{4} - \frac{1}{4}[\chi_1(R_0) + \chi_1(R_b)] . \tag{3.10}$$

It may be easily verified that χ_b is continuous at $\psi_0 = \pi/2$. We now state the properties of the function χ (χ_0, R_0, ψ_0).

i) For $R_0 = 0$, the expression reduces to the usual one for the radial null geodesics:

$$\chi = \chi_0 + \tfrac{1}{2} \sin^{-1} \alpha^{1/2} R . \tag{3.11}$$

ii) For a fixed value of R_0 and χ_0, χ is an increasing function of ψ_0. Therefore if neutrinos were emitted from a point in all directions at the same time, the neutrino emitted in the radially outward direction ($\psi_0 = 0$) will emerge first while the last to reach the surface will be the one emitted radially inward ($\psi_0 = \pi$).

iii) The dependence of χ_b on χ_0 is purely additive in nature. $\chi_b - \chi_0$ is independent of χ_0. This property is fully exploited in the section dealing with the confinement of the neutrinos from infinity. This completes the discussion of the parameter χ along the null geodesic.

Similar analysis can be followed to evaluate φ along the null geodesic. From equations (3.1) we obtain

$$\left(\frac{dR}{d\varphi}\right)^2 = R^2(1 - \alpha R^2)\left(\frac{R^2}{B^2} - 1\right). \tag{3.12}$$

If we assume that the neutrino starts from φ_0, then the integration leads to the following expression for the coordinate φ:

$$\varphi = \varphi_0 \pm \tfrac{1}{2}[\varphi_1(R) - \varphi_1(R_0)] , \tag{3.13}$$

where

$$\varphi_1(R) = \sin^{-1} \frac{1 + \alpha {R_0}^2 \sin^2 \psi_0 - 2{R_0}^2/R^2 \sin^2 \psi_0}{1 - \alpha {R_0}^2 \sin^2 \psi_0} ,$$

the upper sign to be chosen if $\psi_0 \leq \pi/2$.

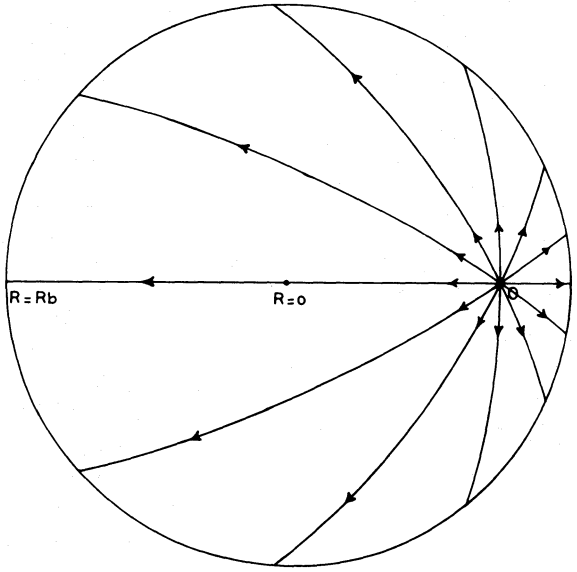

FIG. 1.—The trajectories of neutrinos emitted from an interior point O of the collapsing object and in various directions in the (R, φ)-plane of the Friedmann geometry.

At the boundary $R = R_b$ we have the followings relations:
For $\psi_0 \leq \pi/2$,

$$\varphi_b = \varphi_0 - \tfrac{1}{2}[\varphi_1(R_b) - \varphi_1(R_0)] . \tag{3.14a}$$

For $\psi_0 \geq \pi/2$,

$$\varphi_b = \varphi_0 + \pi/2 + \tfrac{1}{2}[\varphi_1(R_b) + \varphi_1(R_0)] , \tag{3.14b}$$

where φ_b denotes the φ coordinate of the neutrino when it reaches the surface $R = R_b$. The trajectories are plotted in the (R, φ)-plane in Figure 1. One observes that the neutrinos appear to experience a bounce.

This ends the discussion of the neutrino trajectories in the Robertson-Walker spacetime.

b) *The Matching Conditions*

We give only a brief account as to how the matching of the metric is to be carried out at the boundary $R = R_b$. Spherical symmetry of both the geometries enables us to choose the spherical coordinates θ and φ to be common to both of them. We need only match the radial and the time coordinates. The comparison of the spherical portion of the line-elements immediately furnishes one relation:

$$r = RS(T) . \tag{3.15}$$

Since our aim is to continue the null geodesic to the Schwarzschild domain, we require evaluation of the four partial derivatives $\partial r/\partial R$, $\partial r/\partial T$, $\partial t/\partial R$, and $\partial t/\partial T$ at the boundary, in order to convert the components of the tangent vector k^α in the Robertson-Walker geometry to the ones in the Schwarzschild geometry. The first two partial derivatives mentioned can be directly obtained from equation (3.15). The derivatives $\partial t/\partial R$ and $\partial t/\partial T$ can be obtained by setting

$$dT^2 - S^2(T)\frac{dR^2}{1 - \alpha R^2} = \left(1 - \frac{2m}{r}\right)dt^2 - \left(1 - \frac{2m}{r}\right)^{-1} dr^2$$

in the neighborhood of the boundary and using (3.15). The resulting three equations (consistent) for the two unknowns $\partial t/\partial R$ and $\partial t/\partial T$ may be solved to yield

$$\left.\frac{\partial t}{\partial T}\right|_{R=R_b} = \left(1 - \frac{2m}{r}\right)^{-1}(1 - \alpha R_b{}^2)^{1/2} ,$$
$$\left.\frac{\partial t}{\partial R}\right|_{R=R_b} = \frac{(1 - 2m/r)R_b S}{(1 - \alpha R_b{}^2)^{1/2}}\frac{dS}{dT} \tag{3.16}$$

We have naturally chosen the positive sign for $\partial t/\partial T$ (t should normally increase with T). The derivative $\partial t/\partial R$ is negative as $dS/dT < 0$ after the collapse has begun.

Though not necessary for the computations of this paper, we require to know the relation between t and T for a particle on the boundary, when we intend to compute the energy flux as a function of time. We attempt to find t as a function of χ. Without loss of generality we may assume $t = 0$ when $T = 0$ which implies $\chi = 0$. This means we fix $t = 0$ as the time when the collapse starts. Then it may be obtained by integrating the first of the equations (3.16) or from the fact that the particle on the boundary describes a radial geodesic starting at $r = R_b$, $t = 0$, and with the initial tangent vector given by $(dr/dt)|_{t=0} = 0$. We simply state the relation $t(\chi)$:

$$t = \left(\frac{R_b}{2m} - 1\right)^{1/2} (R_b + 4m)\chi + R_b\left(\frac{R_b}{2m} - 1\right)^{1/2} \sin\chi\cos\chi + 2m \log \frac{(R_b/2m - 1)^{1/2} + \tan\chi}{(R_b/2m - 1)^{1/2} - \tan\chi}. \tag{3.17}$$

c) *Null Geodesics in the Schwarzschild Geometry*

This portion of the discussion has been amply dealt with in the past, but here for the sake of completeness we will mention the relevant results.

We have already seen from the earlier discussion that it is sufficient to consider the geodesics confined to the $\theta = \pi/2$ plane. This hypersurface has the intrinsic geometry described by the expression

$$dS^2 = e^{\nu}dt^2 - e^{-\nu}dr^2 - r^2 d\varphi^2 , \tag{3.18}$$

where

$$e^{\nu} = 1 - 2m/r .$$

The symmetries of the spacetime furnish the following first integrals of the geodesics:

$$e^{\nu}\frac{dt}{d\lambda} = \bar{\Gamma} , \qquad r^2\frac{d\varphi}{d\lambda} = \bar{h} . \tag{3.19}$$

Since the geodesic is null, we have another first integral in $ds = 0$. Equations (3.19) may be used to give the following relation which excludes the affine parameter λ,

$$r^2 e^{-\nu}\frac{d\varphi}{dt} = b , \tag{3.20}$$

where b is the ratio $\bar{h}/\bar{\Gamma}$. Here b is the impact parameter in the *Schwarzschild* geometry. At infinity b reduces to the usual expression $r^2 d\varphi/dt$. Equation (3.20) together with $ds = 0$ gives the following expression for dr/dt:

$$\frac{dr}{dt} = \pm\left(1 - \frac{2m}{r}\right)\left[1 - \frac{b^2}{r^2}\left(1 - \frac{2m}{r}\right)\right]^{1/2} . \tag{3.21}$$

Integrating formally, we have:

$$t - t_0 = \pm\int_{r_0}^{r} \frac{dr}{(1 - 2m/r)[1 - (b^2/r^2)(1 - 2m/r)]^{1/2}} . \tag{3.22}$$

Although the integral in (3.22) cannot be evaluated analytically, its value can be estimated from numerical computations and hence it is possible to plot the function $t(r)$ in the (r, t)-plane.

Qualitatively the geodesics can be discussed from the properties of the effective potential; one may write equation (3.21) in the following way:

$$\left(\frac{dr}{dt}\right)^2 = b^2\left(1 - \frac{2m}{r}\right)^2\left[\frac{1}{b^2} - V^2(r)\right], \tag{3.23}$$

where

$$V^2(r) = \frac{1}{r^2}\left(1 - \frac{2m}{r}\right).$$

In Figure 2, V^2 is plotted as a function of r. It is seen that V^2 has a maximum of $1/(27m^2)$ at $r = 3m$, tends to zero as $r \to \infty$, and vanishes at $r = 2m$. This behavior immediately has the following as its important consequence. Particles with $b \geq 3^{3/2}m$ are confined to the side in which they are initially present, namely either the inside or the outside of the sphere $r = 3m$. For $b < 3^{3/2}m$ the sphere $r = 3m$ does not present any barrier. This property of the Schwarzschild geometry and the null geodesics will play a crucial role in the escape or the confinement of the neutrinos from the observer at infinity.

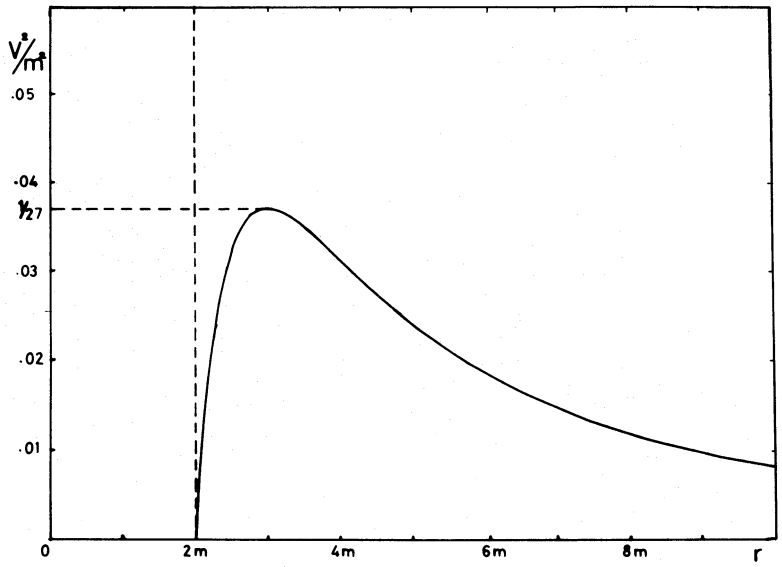

FIG. 2.—The effective potential curve for zero mass particles (null geodesics). The effective potential V^2 possesses a maximum of $1/(27m^2)$ at $r = 3m$ and decays as r tends to infinity.

IV. RELATION BETWEEN THE IMPACT PARAMETERS B AND b

The relation between b and B can be obtained on considering the following situation. Let a neutrino be emitted from R_0 at χ_0 and making an angle ψ_0 with the outward radial direction. Then we immediately have the relation between B and the initial parameters, namely, $B = R_0 \sin\psi_0$. In this section our object lies in finding b as a function of R_0, χ_0, and ψ_0. Since b corresponds to the Schwarzschild domain and R_0, χ_0, and ψ_0 to the Robertson-Walker, we try to connect these quantities by examining the situation at the boundary where both these domains meet. Let k^α be the tangent vector to the null geodesic. We have $k^\alpha k_\alpha = 0$; that is, k^α is a null vector. The components of k^α can be evaluated at the boundary from recalling the geodesic first integrals (3.1):

$$k^0 = \frac{dT}{d\lambda} = \frac{\Gamma}{\cos^2\chi_b},$$

$$k^1 = \frac{dR}{d\lambda} = \frac{\Gamma}{\cos^2\chi_b}\left[(1-\alpha R_b^2)\left(1-\frac{B^2}{R_b^2}\right)\right]^{1/2},$$

$$k^2 = \frac{d\theta}{d\lambda} = 0,$$

$$k^3 = \frac{d\varphi}{d\lambda} = \frac{\Gamma b}{R_b^2\cos^4\chi_b}. \tag{4.1}$$

The component k^0 is the energy of the neutrino. As χ_b is a function of R_0, χ_0, and ψ_0, the components k^α are expressed in terms of these parameters.

If $\bar{k}^\alpha$ denotes the components of the tangent vector to the null geodesic in the Schwarzschild geometry, then $\bar{k}^\alpha$ may be obtained from k^α by the usual vector transformation law. This is possible at the boundary where we have already evaluated the required partial derivatives. For finding the relation between b and B it is only necessary to compute $\bar{k}^0$. At the boundary $R = R_b$ we denote the components of $\bar{k}^\alpha$ in the Schwarzschild coordinates by $\bar{k}_b{}^\alpha$. We then have

$$\bar{k}_b{}^0 = \left(\frac{\partial t}{\partial T}k^0 + \frac{\partial t}{\partial R}k^1\right)\Big|_{\text{boundary}}. \tag{4.2}$$

Using the relations (4.1) and (3.16), we have

$$\bar{k}_b{}^0 = \frac{\Gamma e^{-\nu_b}}{\cos^2\chi_b}[(1-\alpha R_b^2)^{1/2} - \alpha^{1/2}\tan\chi_b(R_b^2 - B^2)^{1/2}]. \tag{4.3}$$

From $e^{\nu}dt/d\lambda = \bar{\Gamma}$ and $\bar{k}_b{}^0 = dt/d\lambda|_b$ we have a relation between Γ and $\bar{\Gamma}$:

$$\bar{\Gamma} = \frac{\Gamma}{\cos^2 \chi_b}[(1 - \alpha R_b{}^2)^{1/2} - \alpha^{1/2} \tan \chi_b (R_b{}^2 - B^2)^{1/2}] . \tag{4.4}$$

In view of the first integrals of the geodesic for $d\varphi/d\lambda$ in both the geometries, we have at the boundary

$$h = R_b{}^2 S_b{}^2 \frac{d\varphi}{d\lambda} = r_b{}^2 \frac{d\varphi}{d\lambda} = \bar{h} . \tag{4.5}$$

Equations (4.4) and (4.5) immediately give the required relation:

$$b = \frac{R_0 \sin \psi_0 \cos^2 \chi_b}{(1 - \alpha R_b{}^2)^{1/2} - \alpha^{1/2} \tan \chi_b (R_b{}^2 - R_0{}^2 \sin^2 \psi_0)^{1/2}} . \tag{4.6}$$

It might at first sight seem that b could have negative values due to the negative sign in the denominator of the expression for b. However, a closer look at the expression shows that for $r_b = R_b \cos^2 \chi_b > 2m$, b remains positive. $R_b \cos^2 \chi_b > 2m$ implies $\tan \chi_b < [(1 - 2m/R_b)/(2m/R_b)]^{1/2}$, which in terms of α becomes $\alpha^{1/2} R_b \tan \chi_b < (1 - \alpha R_b{}^2)^{1/2}$. This immediately gives $(1 - \alpha R_b{}^2)^{1/2} - \alpha^{1/2} \tan \chi_b (R_b{}^2 - R_0{}^2 \sin^2 \psi_0)^{1/2} > 0$. Also b attains higher values for larger R_0 when the neutrinos are emitted from a point closer to the surface of the object. However, the dependence of b on ψ_0 is more complicated. Clearly if $\psi_0 = 0$ or π, then $b = 0$, and the neutrino travels radially. Therefore b possesses at least one maximum in the range $0 \leq \psi_0 \leq \pi$. On the basis of numerous computations we state here that in the early stages of the collapse b has only one maximum. If the collapse is advanced and the neutrinos emerge from the star when its radius is roughly the Schwarzschild radius, then b has two maxima and a minimum in between. The second maximum (with a larger value for ψ_0) plays an important role in the confinement of the neutrinos from the distant observer.

V. SPECTRAL SHIFT

The spectral shift computation plays a pivotal role in the energy considerations of the neutrino flux seen at infinity. In fact, if a large portion of the neutrinos are redshifted, then only a fraction of the energy emitted will be detected at infinity. We analyze this aspect of the problem in this section.

Let the neutrino be emitted with parameters (R_0, χ_0, ψ_0) and received at r by a static observer, whose world line is $(r, \theta, \varphi) =$ constant, in the Schwarzschild geometry. Let ν_e be the frequency of the neutrino emitted as seen by the comoving observer in the Robertson-Walker geometry, and ν_{ob} be the frequency observed at r. Then the spectral shift formula is given by

$$1 + z = \nu_e/\nu_{ob} \tag{5.1}$$

with $\nu_e = k^{\alpha} v_{\alpha}$ where $v_{\alpha} \equiv (1, 0, 0, 0)$ in the Robertson-Walker geometry and

$$\nu_e = k^0 = \frac{\Gamma}{\cos^2 \chi_0} . \tag{5.2}$$

If u^{α} denotes the 4-velocity of the static observer, then

$$\nu_{ob} = \bar{k}^{\alpha} u_{\alpha} , \qquad \text{where } u_{\alpha} = (e^{\nu/2}, 0, 0, 0, 0) ,$$

so that

$$\nu_{ob} = e^{\nu/2} \bar{k}^0 , \tag{5.3}$$

where $\bar{k}^{\alpha}$ is the tangent to the neutrino trajectory at r. From equation (4.3) and the fact that $e^{\nu}\bar{k}^0$ is a constant along the null geodesic we get the required expression for the spectral shift,

$$1 + z = \frac{\nu_e}{\nu_{ob}} = \frac{\cos^2 \chi_b}{\cos^2 \chi_0}[(1 - \alpha R_b{}^2)^{1/2} - (\alpha)^{1/2} \tan \chi_b (R_b{}^2 - R_0{}^2 \sin^2 \psi_0)^{1/2}]^{-1} e^{\nu/2} . \tag{5.4}$$

The spectral shift $1 + z$ easily falls into three separate constituent portions each of which possesses some physical significance,

$$1 + z = (1 + z_c)(1 + z_d)(1 + z_s) , \tag{5.5}$$

where

$$1 + z_c = \frac{\cos^2 \chi_b}{\cos^2 \chi_0}$$

$$1 + z_d = [(1 - \alpha R_b{}^2)^{1/2} - (\alpha)^{1/2} \tan \chi_b (R_b{}^2 - R_0{}^2 \sin^2 \psi_0)^{1/2}]^{-1} ,$$

$$1 + z_s = e^{\nu/2} = (1 - 2m/r)^{1/2} .$$

The quantity $1 + z_c$ may be referred to as the cosmological blueshift. It is known that in the expanding universe particles lose energy in proportion to the expansion; the reverse is to be expected for the collapsing situation. The quantity $1 + z_d$ is the Doppler shift due to the retreating surface of the collapsing star. An observer instantaneously coinciding with the surface of the star and who is at rest in the Schwarzschild geometry would record a Doppler shift if a neutrino were emitted from the surface at the same time. The quantity $1 + z_s$ is the familiar Schwarzschild gravitational redshift where the neutrino loses energy in climbing out of the gravitational potential well.

VI. BACKWARD EMISSION

The notion of backward emission is not new to the subject of collapsing objects. This process was first discussed by Jaffe (1969) in connection with the optical appearance of a spherically symmetric collapsing star. The optical appearance of a collapsing star was dealt with earlier by several authors. Ames and Thorne (1968) have extended the analysis of Podurets (1964). Jaffe (1969) first pointed out that one must also take into account photons emitted tangentially to the surface as seen by an observer at rest in the frame of the collapsing surface of the star. This point was further analyzed by Lake and Roeder (1979). All these papers deal with photons being emitted from the surface of the star. The entire analysis of null geodesics emanating from the surface of the star is carried out in the Schwarzschild geometry. However, our picture extends to the interior of the star in which the neutrinos are emitted and also propagate. Therefore our study deals with the behavior of null geodesics which start in the Robertson-Walker geometry and emerge and continue into the Schwarzschild geometry. The problem therefore consists in the computation of null geodesics in both these geometries. If we restrict ourselves to the surface and consider null geodesics with $\psi_0 \leq \pi/2$, then our results would tally with the earlier mentioned work on photons.

We now explain the process of backward emission. Let us for the time being restrict ourselves to the surface of the collapsing star. The notion can be extended to the interior of the star in an obvious way. A particle emitted radially and traveling with the velocity of light (a zero-mass particle) will continue its outward radial motion in the Schwarzschild domain, as is apparent from the earlier discussion. But let us consider the fate of the particle emitted tangentially ($\psi_0 = \pi/2$) to the surface. The particle would have $dR/d\lambda = 0$ initially; but as the surface is collapsing, the particle possesses a negative radial component of velocity as seen by the static observer in the Schwarzschild geometry. Therefore such a particle would have $dr/d\lambda < 0$ at the boundary on emission. The particle is said to be backward emitted. All particles emitted from the interior of the star which have a negative radial component to their velocities in the Schwarzschild geometry on reaching the boundary are said to be backward-emitted. The others with $(dr/d\lambda)|_{\text{boundary}} > 0$ will be said to be forward-emitted.

Consider a neutrino being emitted with $\psi_0 = 0$ (emitted radially outward) from the surface. This particle will have $(dr/d\lambda)|_b > 0$, where the subscript b denotes the value of the quantity at the boundary. Also, as we have argued earlier, for a neutrino emitted from the surface with $\psi_0 = \pi/2$, $(dr/d\lambda)|_b < 0$. But as $(dr/d\lambda)|_b$ is a continuous function of ψ_0, $(dr/d\lambda)|_b = 0$ for some $\psi_0 = \psi_m$ where $0 < \psi_m < \pi/2$. [The subscript m denotes that b has a maximum value compared to other values of b at the same Schwarzschild coordinate, $b = r(1 - 2m/r)^{-1/2}$]. Therefore when $\psi < \psi_m$ the neutrinos are forward-emitted. For $\psi > \psi_m$, at least for values of ψ_0 up to $\gtrsim \pi/2$, the neutrinos are backward-emitted. Also it is apparent that a neutrino emitted with $\psi_0 = \pi$ directed radially inward will come out from the other side and will be forward emitted (if the black hole has not already formed). Such a neutrino will have $dr/d\lambda > 0$. Applying continuity arguments once again, for a value of $\psi_0 = \psi_m'$, the neutrinos emitted with $\psi_0 > \psi_m'$ will be forward-emitted. For $\psi_m < \psi_0 < \psi_m'$, backward emission occurs. The situation has been shown in Figure 3. In the three dimensional picture the angles ψ_m and ψ_m' are the half angles of the cones which decide the forward and backward emission. The vertex of the cones is the point of emission of the neutrinos.

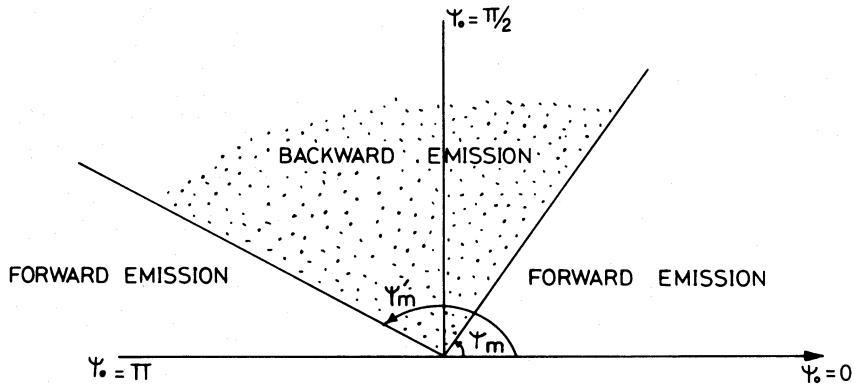

FIG. 3.—The figure depicts the phenomenon of backward emission from a given point $R = R_0$ and at a fixed epoch $\chi = \chi_0$. The dotted region $\psi_m < \psi_0 < \psi_m'$ corresponds to neutrinos which are backward-emitted. The rest of the directions, $0 < \psi_0 < \psi_m$ and $\psi_m' < \psi_0 < \pi$, correspond to neutrinos being forward-emitted.

The arguments given above can be extended to the interior without any variation, but care must be taken to see whether backward emission occurs at all from a given interior point. Backward emission is guaranteed to occur for a point on the surface. The situation is roughly similar for a point close enough to the surface. In general ψ_m and ψ_m' are functions of R_0, χ_0, and R_b. One can determine ψ_m and ψ_m' by noting that $(dr/d\lambda)|_b(\psi_m)$ and $(dr/d\lambda)|_b(\psi_m')$ vanish. This implies that the Schwarzschild impact parameter b has the value

$$b = r_b(1 - 2m/r_b)^{-1/2}\,, \tag{6.1}$$

where $r_b = R_b \cos^2 \chi_b$, the Schwarzschild radial coordinate of the surface of the star. Let ψ_b be the value of ψ when a neutrino emitted with parameters (χ_0, R_0, ψ_0) reaches the boundary. The quantity ψ_b is given by the relation $R_b \sin \psi_b = R_0 \sin \psi_0$, b attains a maximum as a function of ψ_b if the neutrino were emitted at either of the angles ψ_m and ψ_m', and hence they are the solutions of the equation

$$\frac{db}{d\psi_b} = 0\,. \tag{6.2}$$

Equation (6.2) immediately furnishes the following relation:

$$\left(\frac{2m}{R_b}\right)^{1/2} \tan \chi_b - \left(1 - \frac{2m}{R_b}\right)^{1/2} \cos \psi_b = 0\,. \tag{6.3}$$

Removing square roots by multiplying by a positive factor, we define the function F by

$$F = \left(1 - \frac{2m}{R_b}\right)\left(1 - \frac{R_0^2}{R_b^2} \sin^2 \psi_0\right) - \frac{2m}{R_b} \tan^2 \chi_b \tag{6.4}$$

The solutions for ψ_0 in the equation $F = 0$ determines ψ_m and ψ_m'. All the properties of the process of backward emission can be obtained by examining F as a function of χ_0, ψ_0, and R_0. We list some of its useful properties:

i) For $\psi_0 = 0$ and π we have $F > 0$ if $r_b > 2m$ for $\psi_0 = 0, \pi$. Radially directed neutrinos are forward-emitted.

ii) For $R_0 = 0$, $F > 0$ if $r_b > 2m$. All the neutrinos emitted from the center of the star must be forward-emitted if the black hole has not already formed when they arrive at the surface.

iii) where $R = R_b$, the expression for F reduces to

$$F = \left(1 - \frac{2m}{R_b}\right)\cos^2 \psi_0 - \frac{2m}{R_b} \tan^2 \chi_b\,.$$

For $\psi_0 \leq \pi/2$ we have $\chi_b = \chi_0$. The solution for ψ_m can be explicitly obtained in this case:

$$\cos \psi_m = \left(\frac{2m}{R_b - 2m}\right)^{1/2} \tan \chi_0\,, \tag{6.5}$$

where $\psi_m < \pi/2$ for $\chi_0 > 0$.

When $\psi_0 = \pi/2$, we have

$$F = -\frac{2m}{R_b} \tan^2 \chi_0 < 0\,.$$

However, an explicit formula cannot be obtained for ψ_m' even in this case, for $\psi_m' > \pi/2$ and consequently χ_b is a complicated function of ψ_0 and this reflects on F.

The above properties of F show that backward emission must occur from the surface. It was also shown that there is no backward emission from the center. Therefore for a given value of $\chi > 0$ there is a value of $R = R_1$ at which there is a transition from the backward emission zone to the purely forward emission zone. For $R_0 > R_1$ there are values of ψ_0 for which the neutrinos are backward-emitted while for $R_0 < R_1$ all neutrinos irrespective of the value of ψ_0 are forward-emitted. The points $R < R_1$ form a forward emission sphere. We observe that R_1 is a function of χ and R_b. It is easily seen that $R_1 = R_b$ when $\chi = 0$ and $R_1 = 0$ when $r_b = R_b \cos^2 \chi_b = 2m$. R_1 is a monotonic decreasing function of χ for a given value of R_b. R_1 may be obtained from the function F in the following way. As R_0 decreases from the value of R_b, the two roots of $F = 0$, ψ_m, and ψ_m' start coming close together [the curve $F = 0$ moves up in the (ψ, F)-plane] until at the limiting value of $R_0 = R_1$ they coincide: $\psi_m = \psi_m' = \psi_1$ [the curve $F = 0$ is tangential to the ψ-axis in the (ψ, F)-plane]. Clearly ψ_1 is also a function of χ and R_b. For a fixed value of $R_b = 100m$ we have plotted R_1 as a function of χ in Figure 4. From the expression for F we can easily show that $\psi_1 > \pi/2$. We have ψ_1 as a solution of $F = 0$ and $dF/d\psi_0 = 0$:

$$\frac{dF}{d\psi_0} = -\frac{2R_0^2}{R_b^2}\left(1 - \frac{2m}{R_b}\right) \sin \psi_0 \cos \psi_0 - \frac{4m}{R_b} \tan \chi_b \sec^2 \chi_b \frac{d\chi_b}{d\psi_0}\,. \tag{6.6}$$

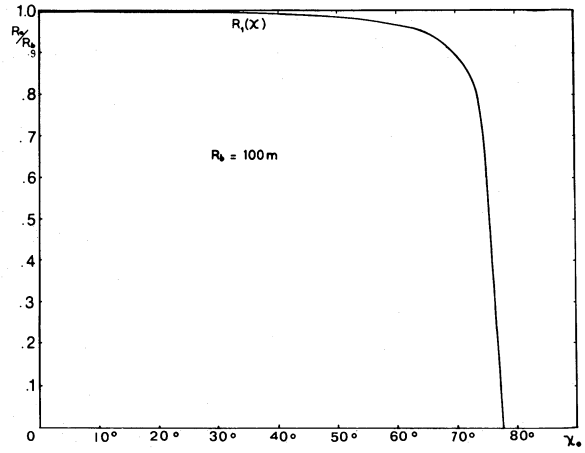

FIG. 4.—The quantity R_1/R_b plotted as a function of the epoch χ_0 for $R_b = 100m$. At a fixed epoch χ_0 for $R < R_1$, all the neutrinos are emitted in the forward direction, while for $R > R_1$ there exists a range of directions for which the neutrinos are backward emitted.

Since $d\chi_b/d\psi_0 > 0$, the second term is always negative and so $dF/d\psi_0$ can equal zero only when the first term is positive, which is possible only if $\psi_0 > \pi/2$.

There is one simple point which must be mentioned. Can the backward-emitted neutrino enter the star? One computes the trajectory of the neutrino emitted with $\psi_0 = \pi/2$ from the surface, for this has the most likelihood of reentering the star. However, on calculating the t-coordinates of both the surface and the neutrino one can check that the surface falls faster.

VII. THE ESCAPE AND THE CONFINEMENT OF NEUTRINOS FROM INFINITY

In the static case as shown by Kembhavi and Vishveshwara, trapping of the neutrinos can occur only if the radius of the star lies between $2m$ and $3m$. This can be easily seen from the effective potential profile depicted in Figure 2. The peak of the effective potential occurs at $r = 3m$ at which the impact parameter b has the value $(3)^{3/2}m$. Particles with $b > (3)^{3/2}m$ and in the region $2m < r < 3m$ cannot escape to infinity. However, in the case of a collapsing star the situation is different since the phenomenon of backward emission is present. Particles may fall into the black hole even though they may be emitted from a point whose radial coordinate is greater than $3m$. This happens when both the conditions mentioned below are satisfied:

i) *There is backward emission* ($F < 0$).
ii) $b < (3)^{3/2}m$.

For the second condition to be satisfied it is necessary that the collapse of the star should be sufficiently progressed that the radius of the star is small. If the star has already collapsed within $3m$ when the neutrino emerges from the star, it is comparatively easily swallowed up in the resulting black hole. The neutrino cannot escape to infinity if either or both of the conditions are satisfied:

i) *The neutrino is backward-emitted* ($F < 0$).
ii) $b > 3^{3/2}m$.

In the first case there is no way to reverse the infall of the neutrino; hence it is gobbled up by the eventual black hole. In the second case the neutrino, even if it is emitted with $dr/d\lambda|_b > 0$, will bounce at the effective potential barrier and then fall into the black hole.

a) The Truth Table

The confinement of the neutrinos can be conveniently and lucidly expressed with the aid of a "truth table" which states whether the neutrino is confined or not according to the truth or the falsity of the following three statements:

A. $r_b < 3m$, where r_b is the Schwarzschild coordinate of the surface of the star when the neutrino reaches the surface $r_b = R_b \cos^2 \chi_b$.
B. $F < 0$.
C. $b < (3)^{3/2}m$.

TABLE 1

TRUTH TABLE FOR NEUTRINO CONFINEMENT

$r_b < 3m$ (A)	$F < 0$ (B)	$b < 3(3m)^{1/2}$ (C)	Confinement (D)
1	1	1	1
1	1	0	1
1	0	1	0
1	0	0	1
0	1	1	1
0	1	0	0
0	0	1	0
0	0	0	0

Let D be the condition that the neutrino is confined from infinity (see Table 1), where 1 under a given column indicates that the statement is true while 0 denotes the falsity. If we actually assign these numerical values to the conditions A, B, C, and D, then D can be expressed as a arithmetic expression in A, B, and C:

$$D = A(1 - C) + BC . \tag{7.1}$$

Brevity is another advantage in using the truth table. For example, if a null trajectory satisfies condition A but not B and C, then from the truth table we will assign to it the truth value 100. This type of terminology saves space. The scheme is very useful in studying the escape or the confinement of the neutrino from infinity. Each of the quantities r_b, F, and b appearing in the three conditions are functions of the initial parameters R_0, χ_0, and ψ_0; therefore the conditions A, B, and C impose nonholonomic constraints on these parameters. The conditions A, B, and C will divide the (R_0, χ_0, ψ_0)-space into regions in which D is either true or false. We will study these constraints by fixing the values of either one or two of the parameters and varying the remaining. It is convenient and fruitful to fix $R_0 = R_b$ in the beginning and then relate the already obtained results to an interior point $R_0 < R_b$. Clearly R_0, χ_0, and ψ_0 determine a unique null geodesic. But the values of R_0, χ_0, and ψ_0 at other points on the null geodesic may also be used as initial parameters which would determine the same null geodesic. The null geodesics furnish an equivalence relation on the space of the initial parameters (R_0, χ_0, ψ_0). In particular one may choose the initial parameters when the null geodesic reaches the boundary $R = R_b$. Since the confinement properties for the surface case would have already been discussed, the results for the interior point can be deduced.

b) *The Surface Case* $R_0 = R_b$

The entire analysis of the confinement mechanism of the neutrinos. is dependent on the conditions A, B, and C mentioned above, which involve constraints on the functions r_b, F, and b. Therefore it seems useful to adopt a scheme which displays all these functions simultaneously and which compares their relative behavior. We already have fixed $R_0 = R_b$, and now we fix χ_0 for the time being so that the only variable is ψ_0. We restrict ourselves to neutrinos being emitted simultaneously at $\chi = \chi_0$ from a point on the surface. The parameters r_b, F, and b are functions of ψ_0 only. We make use of the fact that χ_b as a function of ψ_0 is strictly increasing in the range $\pi/2 \leq \psi_0 \leq \pi$, that is, the neutrinos emitted with a greater value of ψ_0 emerge out of the star at a later stage. Hence $r_b = R_b \cos^2 \chi_b$ as a function of ψ_0 is monotonic decreasing on $[\pi/2, \pi]$. Therefore, b and F may be regarded as functions of r_b instead of ψ_0. In the discussion which follows we consider the (r_b, b)-plane. The function $b(r_b)$ defines a curve in the plane, in future referred to as a b-curve. $F = 0$ determines a value of r_b. One can display $F = 0$ by a vertical line drawn at that particular value of r_b which demarcates the forward-emitted $(F > 0)$ neutrinos from the backward-emitted $(F < 0)$ neutrinos. If all the neutrinos emerge from the star before r_b reaches $2m$, then the $F = 0$ line lies in the region $r_b > 2m$. This may be seen by observing that $F > 0$ for $\psi_0 = \pi$ and $F < 0$ for $\psi_0 = \pi/2$. In this picture all the three functions which decide the confinement are displayed.

The effect of change in χ_0 is to vary the b curves and alter the position of the $F = 0$ line on the r_b axis. The b curves should be compared with the line $b = (3)^{3/2}m$.

We possess now all the machinery necessary to describe the process of confinement of the neutrinos emitted from the surface at various stages of the collapse. At the beginning of the collapse there is no confinement. If R_b is quite large—as it may be in realistic situations—at the beginning of the collapse the radius of the star is also quite large, and this results in $b_{max} \sim r_b \gg m$ which means that the conditions for confinement are not satisfied. In fact, if the neutrino which emerges last from the star comes out when the radius of the star is greater than $3m$, then there can be no confinement. This fact may be used to obtain a rough upper bound on the radius of the star when the neutrino was emitted, for confinement to be possible. The upper bound is obtained as follows. The last emerging neutrino must be emitted with $\psi_0 = \pi$. We now impose the condition that $r_b = 3m$ for this neutrino, that is, the neutrino should emerge when the radius of the star is $3m$.

This many data are sufficient to compute the epoch of emission and hence the radius of the star when the neutrino was emitted. We have, for $\psi_0 = \pi$,

$$\chi_b = \chi_0 + \pi/4 - \tfrac{1}{2} \sin^{-1} (1 - 2\alpha R_b^2) . \tag{7.2}$$

We now set $R_b \cos^2 \chi_b = 3m$. These equations can be solved for χ_0. We merely state the result,

$$r_b = R_b \cos^2 \chi_0 = m\left\{2 \times 6^{1/2} - \left[\left(1 - \frac{3m}{R_b}\right)\left(1 - \frac{2m}{R_b}\right)\right]^{1/2} + 5 - \frac{12m}{R_b}\right\} . \tag{7.3}$$

For $R_b \gg m$,

$$r_b = R_b \cos^2 \chi_0 \approx [(2 \times 6)^{1/2} + 5]m \approx 9.9 \text{ m} .$$

Equation (7.3) shows that $R_b \cos^2 \chi_0$ is an increasing function of R_b, and hence we can make the general statement (for all R_b) that confinement from infinity of a neutrino emitted from the surface cannot occur if the radius of the star is greater than $[(2 \times 6)^{1/2} + 5]m$.

This suggests that the interesting situation arises only when the b-curves cross over into the $r_b < 3m$ region. One such curve is shown in Figure 5 for $\chi_0 = 73°.15$ and $R_b = 100m$. The curve does not go above the line $b = (3)^{3/2}m$ in the region $r_b < 3m$. The neutrino has been emitted slightly after the critical epoch χ_0 defined by equation (7.3). The $F = 0$ line lies in the region $r_b > 3m$ so that $F > 0$ in the region $2m < r_b < r_{b0}$ where r_{b0} is the solution of $F = 0$. Clearly none of the confinement conditions is satisfied. This shows that the radius determined by (7.3) is only a *rough* upper bound. Another property of the b-curve is that at r_{b0} the value of b is greater than or equal to $(3)^{3/2}m$. The condition $F = 0$ implies that the neutrino on emerging from the surface in the Schwarzschild geometry has zero radial component and hence $b = r_b(1 - 2m/r_b)^{1/2}$. It is then easy to check that the function $r_b(1 - 2m/r_b)^{-1/2}$ attains a minimum of $3^{3/2}m$ at $r_b = 3m$ and remains greater than the minimum value for $r_b \neq 3m$. This property is useful as a guideline in tracing the b-curves.

If we advance the epoch of emission χ_0, the b-curve grows in height in the region $r_b < 3m$ until at a critical epoch the curve develops a maximum and touches the line $b = 3^{3/2}m$. A further small increment to the value of χ_0 leads to the b-curve crossing the line $b = 3^{3/2}m$, so that the maximum value of b is greater than $3^{3/2}m$. The $F = 0$ line still lies in the region $r_b > 3m$, but now we notice from the truth table that the condition 100 is satisfied for some small range of values of ψ_0 and these neutrinos cannot escape to infinity. The confinement occurs for values of r_b lying in the interval whose end points are determined by the b-curve intersecting the line $3^{3/2}m$ in the region $r_b < 3m$. This interval on the r_b-axis corresponds to values of ψ_0 lying in some subinterval of $[\pi/2, \pi]$. In the three dimensional picture, the confinement process begins with the directions of confinement lying between two coincident cones with their half-angles lying between $\pi/2$ and π measured from the outward radial direction. As the collapse proceeds, the cones tend to enclose a larger solid angle,

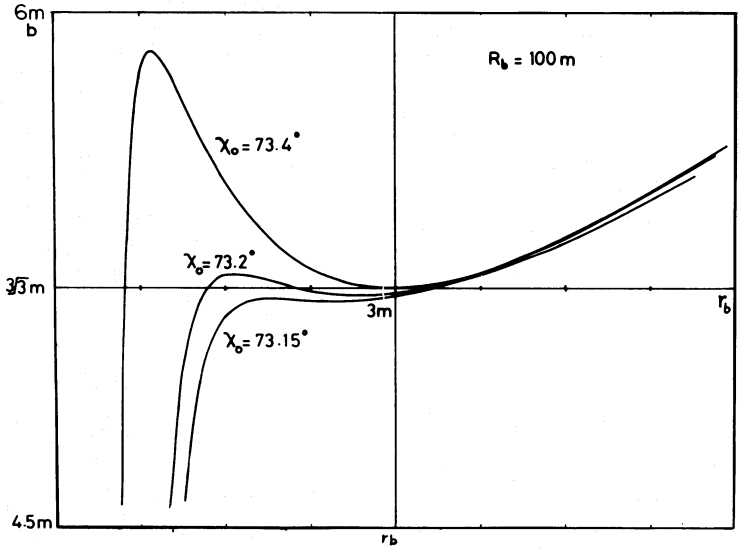

FIG. 5.—The figure shows the b-curves in the initial stages of the confinement process. The Schwarzschild impact parameter b is plotted as a function of r_b for various values of the epoch χ_0. The neutrinos are emitted from the surface of the object. The value of the surface radius is $R_b = 100m$. The least value of r_b shown in the figure is $2m$. Those portions of the curves are shown ($r_b \gtrsim 2m$) which are relevant to the initial stages of the confinement process. For the lowest value of χ_0 shown (73°.15) there is no confinement. At a slightly later epoch (73°.2) the b-curve goes over the line $b = (3)^{3/2}m$. Therefore in a small range of directions confinement occurs. The third case of $\chi_0 = 73°.4$ shows even a later stage of the confinement process. The b-curve has a maximum for $r_b < 3m$ and a minimum at $r_b = 3m$. This is the critical epoch at which the confinement conditions listed in the truth table undergo various changes.

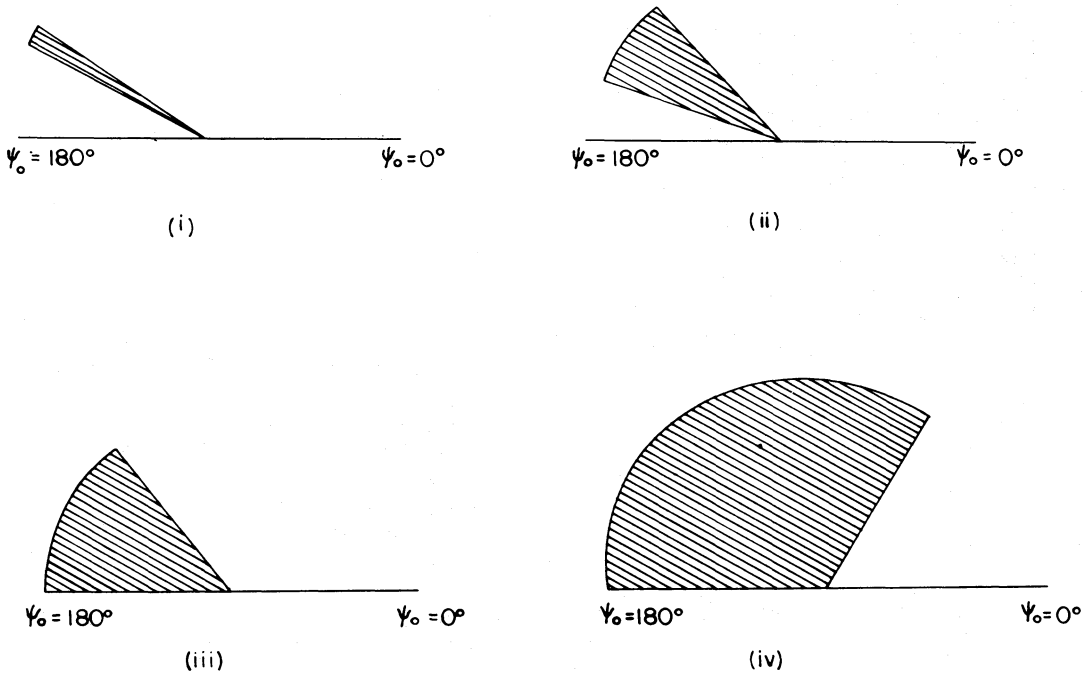

FIG. 6.—The darkened regions in the figure show the range of directions in the angle ψ_0 for which confinement occurs. The four figures (i), (ii), (iii), and (iv) correspond to epochs in the progressive stages of the collapse. In cases (i) and (ii) the confinement directions are bounded by two cones. In (iii) and (iv) there is only one cone which decides the directions of confinement.

with the outer cone moving outward and the inner cone closing in. A typical such half angle of the coincident cones for $R_b = 100m$ is about 159°. The entire confinement process is shown in the various stages of collapse in Figures 5 and 6. Figure 5 shows the b-curves for various values of the epochs when the confinement process just begins, while Figure 6 depicts the actual directions in which the confinement occurs. The first diagram in Figure 6 is relevant to the above discussion. The exact analytical expression for the epoch and the half-angle when the cones are coincident seems difficult, though desirable, to obtain.

The next change in the confinement conditions occurs when the $F = 0$ line coincides with the $r_b = 3m$ line. The b-curve has a minimum at $r_b = 3m$ and touches the line $b = 3^{3/2}m$ at this point. For $r_b < 3m$ the b-curve has a maximum and then falls to zero for a value of r_b which is greater than $2m$. The directions of confinement correspond to an interval on the r_b-axis whose lower end point is the intersection of the b-curve with the line $b = 3^{3/2}m$ and the upper limit is $3m$. The twin cones now encompass a larger solid angle of confinement directions. We give the exact analytical expression for the epoch,

$$\cos^2 \chi_0 = \frac{x}{(3 - 4x)}[-Q/2 + (Q_1 Q_2)^{1/2}], \tag{7.4}$$

where

$$Q = 72x^3 - 174x^2 + 142x - 39, \quad Q_1 = 36x^3 - 99x^2 + 90x - 27, \quad Q_2 = 36x^3 - 75x^2 + 52x - 12,$$

and $x = 2m/R_b$. For $R_b \sim 100m$, $r_b = R_b \cos^2 \chi_0 \sim 8m$. The next stage in the collapse is when the $F = 0$ line lies between $r_b = 2m$ and $r_b = 3m$. The b-curve now has characteristics somewhat similar to the one when the confinement has just begun; but now, as the $F = 0$ line lies in the region $r_b < 3m$, $F < 0$ to the right of this line, which leads to greater confinement. For $F > 0$ the condition 100 and for $F < 0$ the conditions 110, 111, and 011 are responsible in preventing the neutrinos from escaping to infinity. The region of the confinement on the r_b-axis is further extended to $r_b > 3m$, and the lower limit of the interval decreases further. The two cones still exist—that is, the larger half-angle has not still attained the value $\psi_0 = \pi$ though the solid angle between the cones is considerably larger.

The stage which we consider next occurs when the $F = 0$ line coincides with the line $r_b = 2m$. At this stage only one cone survives, the other cone reaches the half-angle $\psi_0 = \pi$. Therefore the confinement directions lie in a single cone pointing inward. This epoch may be characterized by observing that a neutrino emitted at this epoch with $\psi_0 = \pi$ reaches the

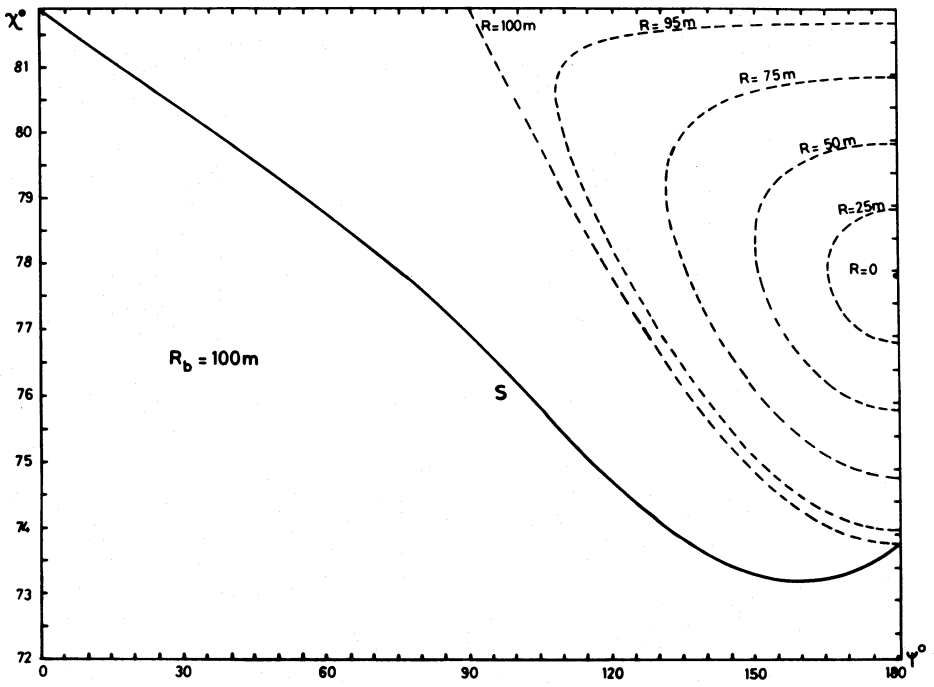

FIG. 7.—The confinement process is depicted in the figure for a wide range of the initial parameters (R_0, χ_0, ψ_0) and $R_b = 100m$. The unbroken curve S determines the confinement process for the neutrinos emitted from the surface $R_0 = R_b$. For the choice of the parameters χ_0, ψ_0 and $R_0 = R_b$ the neutrino is confined if and only if the point (ψ_0, χ_0) lies above the curve S. The dashed curves describe the confinement process for the interior points of the collapsing star. The curves are drawn for the fixed value of $\chi_0 = \chi_f = 81°.87$ obtained from the relation $R_b \cos^2 \chi_0 = 2m$. The curves for other values of χ_0 are obtained by merely translating the given curves in the vertical direction along the χ_0-axis by the amount $\chi_0 - \chi_f$. A neutrino emitted from R_0 at χ_0 is confined if the dashed curve corresponding to R_0 and χ_0 lies in the region above the curve S. The range of angles ψ_0 corresponding to the curve lying within this region determine the directions of confinement.

opposite surface when the star collapses to the radius $2m$. This epoch may be readily computed by a procedure similar to the one employed in obtaining (7.4); we have

$$r_b = R_b \cos^2 \chi_0 = 8m(1 - 2m/R_b) . \tag{7.5}$$

The situation is shown in Figure 6(iii).

After this epoch the half-angle of the cone of confinement $(\pi - \psi_0)$ steadily increases with continued collapse until all directions are exhausted when the star reaches the Schwarzschild radius $2m$. The situation is shown in Figure 6(iv) at an intermediate stage before the star reaches the radius $2m$. At $r_b = 2m$, the cone degenerates into the line $\psi_0 = 0$. This we refer to as total confinement. The half-angle of the cone becomes $\pi/2$ when the radius of the star is $(3)^{3/2}m(1 - 2m/R_b)$.

The entire process of the confinement as a function of the collapse parameter χ_0 is shown in the (ψ, χ)-plane in Figure 7. A neutrino emitted from $R = R_b$ and $\chi = \chi_0$ and $\psi = \psi_0$ will be confined from infinity if the point lies in the region above the undotted curve S. The presence of the minimum of the curve shows that there is twin cone confinement. This may be explained as follows. Any given epoch $\chi = \chi_0$ represents a horizontal line in the (ψ, χ)-plane. Confinement in some directions will occur at this epoch if and only if the line $\chi = \chi_0$ crosses the curve S. In the beginning of the collapse the line $\chi = \chi_0$ is far below the curve in the (ψ, χ)-plane; and as the collapse proceeds, this line moves upward. At a critical epoch the line touches the curve S at the minimum and the confinement process begins. A little later the line $\chi = \chi_0$ intersects S at two points whose ψ coordinates are ψ_1 and ψ_2. This is possible because the curve S possesses a minimum. For $\psi_1 < \psi < \psi_2$ the neutrinos are confined from infinity. At a later stage when χ exceeds χ_1 given by $R_b \cos^2 \chi_1 = 8m(1 - 2m/R_b)$, the line $\chi = \chi_0$ intersects the curve S at only one point, say ψ_1. In this case neutrinos are confined for values of $\psi > \psi_1$, which shows that only a single cone of confinement exists for this advanced epoch. This concludes the discussion of neutrinos emitted from the surface.

c) *Generalization to the Emission of Neutrinos from the Interior of the Object*

Let a neutrino be emitted from a point $R_0 < R_b$. As the interior metric harbors a repulsive potential, the neutrino must arrive at the boundary. We now propose to relate the parameters R_0, χ_0, and ψ_0 to those on the boundary. Two possibilities exist in the choice of the parameters at the boundary, as the null geodesic when produced into the past and the future would intersect the surface at two points. More specifically, if we denote the values of χ and ψ at the boundary

by χ_{R_0} and ψ_{R_0}, then we could either choose $\chi_{R_0} < \chi$ or $\chi_{R_0} > \chi_0$. We make the following choice: We choose the point on the boundary where the null geodesic intersects to lie to the past of χ_0, that is, $\chi_{R_0} < \chi_0$. From the foregoing discussion we have the following relations between the actual and the boundary parameters.

For $\psi_0 \leq \pi/2$,

$$\chi_{R_0} = \chi_0 - \frac{\pi}{4} + \frac{1}{4}\left(\sin^{-1}\frac{1 + \alpha R_0{}^2 \sin^2\psi_0 - 2\alpha R_0{}^2}{1 - \alpha R_0{}^2 \sin^2\psi_0} - \sin^{-1}\frac{1 + \alpha R_0{}^2 \sin^2\psi_0 - 2\alpha R_b{}^2}{1 - \alpha R_0{}^2 \sin^2\psi_0}\right)$$

For $\psi_0 \geq \pi/2$,

$$\chi_{R_0} = \chi_0 - \frac{1}{4}\left(\sin^{-1}\frac{1 + \alpha R_0{}^2 \sin^2\psi_0 - 2\alpha R_0{}^2}{1 - \alpha R_0{}^2 \sin^2\psi_0} - \sin^{-1}\frac{1 + \alpha R_0{}^2 \sin^2\psi_0 - 2\alpha R_b{}^2}{1 - \alpha R_0{}^2 \sin^2\psi_0}\right)$$

and

$$\psi_{R_0} = \sin^{-1}\left(\frac{R_0}{R_b}\sin\psi_0\right),$$

where we choose the inverse trignometric function to be greater than $\pi/2$, i.e., $\psi_{R_0} \geq \pi/2$.

In the (ψ, χ)-plane the equations (7.6) give a parametric representation of a curve in the range $0 \leq \psi_0 \leq \pi$ for each fixed value of R_0. These curves provide a complete picture of the confinement process within the collapsing object. Figure 7 shows the dashed curves for various values of R_0, with $R_b = 100m$; since χ_0 is only an additive constant, it has been chosen arbitrarily by the relation $R_b \cos^2 \chi_0 = 2m$. In drawing the curves, the actual value of χ_0 is not very important because any variation in χ_0 merely displaces the curve in the vertical direction. This can be easily seen from equations (7.6). As has been mentioned, the dependence of χ_{R_0} on χ_0 is purely additive in character, and also ψ_{R_0} does not depend on χ_0 at all. The examination of the situation is thus rendered simpler.

The dotted curve drawn for $R_0 = R_b$ may be thought of as a limiting case when R_0 tends to R_b. However, the case $R_0 = R_b$ may also be included in the general discussion carried out for all values of R_0. We first discuss the properties of the curves defined by (7.6) and their implications.

a) For each fixed value of R_0, the curve is convex and it has zero slopes at both the points where $\psi_{R_0} = \pi$. This immediately has the consequence that the nature of the confinement process for an interior point is broadly similar to the one for a point on the surface. If any portion of the dotted curve drawn for a value of R_0 lies in the region above the curve S, then the neutrinos emitted with parameters ψ_0 and χ_0 corresponding to that portion of the curve experience confinement. We also saw that any variation in χ_0 only displaces the curve vertically. In case the neutrinos are emitted at the beginning of the collapse, the curve is well below the curve S and hence none of the neutrinos is confined. If the value of χ_0 is allowed to increase with the progress of collapse, at a critical epoch the dotted curve touches the curve S. At a slightly later stage in the collapse the dotted curve intersects the curve S at two points leading to confinement between two cones. With further increase in χ_0 the dotted curve intersects S at only one point, and so the two cones are reduced to a single cone. This is very similar to the situation of the surface. As χ_0 increases, the cone of confinement encloses a steadily larger solid angle until total confinement occurs. For $R_0 < R_b$ total confinement occurs *before* the object reaches its Schwarzschild radius.

b) The dotted curves for various values of R_0 form a nested sequence. A dotted curve for a smaller value of R_0 lies completely inside a curve for a larger value of R_0 assuming that the epoch of emission χ_0 is the same in both the cases. This causes the entire confinement process for a smaller value of R_0 to start at later epoch and total confinement to occur earlier as compared to the confinement process for neutrinos emitted from a larger R_0. In fact, for the extreme case for $R_0 = 0$, the dotted curve is a point on the line $\psi = \pi$ and the entire confinement process is instantaneous. The epoch at which this occurs may be computed by observing that a neutrino starting from the center at this epoch should reach the surface when the radius of the star is $2m$. The value of this epoch can be easily determined and is given by

$$\cos^2 \chi_0 = \frac{1}{2}\left[1 - \left(1 - \frac{8m}{R_b}\right)\left(1 - \frac{2m}{R_b}\right)^{1/2}\right]. \tag{7.7}$$

This is also the earliest epoch at which total confinement occurs. As the collapse proceeds, the radius of the sphere of total confinement grows until it becomes equal to the radius of the star when the star crosses the Schwarzschild horizon. Neutrinos emitted within this sphere cannot escape to infinity.

VIII. CONCLUSIONS

In the foregoing investigations of the behavior of neutrinos in a collapsing situation, we have carried out detailed and extensive analysis. It is found that the study provides interesting processes such as the backward emission and the confinement of the geodesics due to black hole formation. It is seen that the confinement process begins when the radius of the star is about $9m$, which is considerably larger than $3m$ obtained in the static situation. The confinement process and the Doppler shift due to the collapse could, in addition to gravitational redshift, reduce the energy of the emitted neutrino

by a large factor. If one is interested in the energy flux at infinity and its time development, backward emission would play an important role in that it would delay the arrival of the neutrino at the distant observer. These aspects of the problem will be considered in a second paper.

In our calculations we have not resorted to any approximation methods. For R_b large, such approximations could be made and further insight gained into the behavior of the null geodesics.

REFERENCES

Ames, W., and Thorne, K. S. 1968, *Ap. J.*, **151**, 659.
Hoyle, F., and Narlikar, J. V. 1964, *Proc. Roy. Soc. A*, **278**, 465.
Jaffe, J. 1969, *Ann. Phys.*, **55**, 374.
Kembhavi, A. K., and Vishveshwara, C. V. 1981, to be published.
Lake, K., and Roeder, R. C. 1979, *Ap. J.*, **232**, 277.
Misner, C. W., Thorne, K. S., and Wheeler, J. A. 1973, *Gravitation* (San Fransisco: Freeman).
Podurets, M. A. 1964, *Astr. Zh.*, **41**, 1090 (English transl. *Soviet Astr.—AJ.*, **8**, 868 [1965]).

S. V. Dhurandhar and C. V. Vishveshwara: Raman Research Institute, Bangalore-560 080, India